Solid-State Dynamics and High-Pressure Studies of a Supramolecular Spiral Gear

Published Version:
Fornasari, L., Olejniczak, A., Rossi, F., D'Agostino, S., Chierotti, M.R., Gobetto, R., et al. (2020). Solid-State Dynamics and High-Pressure Studies of a Supramolecular Spiral Gear. CHEMISTRY-A EUROPEAN JOURNAL, 26(22), 5061-5069 [10.1002/chem.201905744].

Availability:
This version is available at: https://hdl.handle.net/11585/784747 since: 2020-12-18

Published:

DOI: http://doi.org/10.1002/chem.201905744

Solid-State Dynamics and High-Pressure Studies of a Supramolecular Spiral Gear.

Luca Fornasari,[a] Anna Olejniczak,[b] Federica Rossi,[c] Simone d'Agostino,*[a] Michele R. Chierotti,*[c] Roberto Gobetto,[c] Andrzej Katrusiak,*[b] and Dario Braga.[a]

Abstract: The structures and solid-state dynamics of the supramolecular salts of general formula [(12-crown-4)$_2$·DABCOH$_2$](X)$_2$ (where X=BF_4, ClO_4) have been investigated as a function of temperature (from 100 K to 360 K) and pressure (up to 3.4 GPa), through the combination of variable temperature and variable pressure XRD techniques and variable temperature solid-state NMR spectroscopy. The two salts are isomorphous and crystallize in the enantiomeric space groups $P3_22_1$ and $P3_12_1$. All building blocks composing the supramolecular complex display dynamic processes at ambient temperature and pressure. It has been demonstrated that the motion of the crown ethers is maintained on lowering the temperature (down to 100 K) or on increasing the pressure (up to 1.5 GPa) thanks to the correlation between neighboring molecules that mesh and rotate in a concerted manner similarly to spiral gears. Above 1.55 GPa, a collapse-type transition to a lower-symmetry ordered structure, not attainable at a temperature of 100K, takes place, proving, thus, that the pressure acts l ke the means to couple and decouple the gears. The relationship between temperature and pressure effects on molecular motion in the solid state has also been discussed.

Introduction

The study of dynamic reorientational processes in crystals,[1] such as molecular rotations or librations, has challenged scientists for decades in view of the unique nature of these phenomena, subverting the common perception of crystals as static entities.[2][3][4][5][6][7][8] Recently, a renewed interest in the field was driven by the surge of artificial molecular machines. The design of crystalline materials possessing components in rapid motion is considered a promising platform for the development of functional materials ranging from switchable ferroelectrics,[9] to gas and vapor sensors,[10] dielectric constant modulators,[11] birefringence,[12] energy-storage thermal buffers and thermal expansion modulators.[13] The study of molecular rotations has been performed on a variety of solids: molecular crystals,[14] co-crystals and salts,[15] metal organic frameworks (MOFs), inclusion compounds, solid solutions,[16][17] porous organic frameworks[18] and dendritic structures.[19]

The common approach in designing such materials relies on the control of the free volume, i.e. granting the rotary component sufficient void volume in the local environment for the rotation to take place. Indeed, it is generally assumed that the motions are of a biased-Brownian type. The bias being an interplay of steric hindrance, and electronic barrier in the case the rotating molecule is connected to a stationary component via covalent bonds.[20] So, a loosely packed structure is desirable to lower the activation energy for the rotation and hence increase its frequency. We recently showed that weak interactions as well can play a significant role.[21] We reported the dynamics of a supramolecular complex of DABCOH$_2$X$_2$ (X=Cl or Br) and 12-crown-4, in which chains are formed as represented in scheme 1, consisting of the repetition of one molecule of crown ether, one of diprotonated DABCO and counterions. It was observed that labile attachment of the DABCOH$_2^{2+}$ cation bonded, via charge assisted N-H···O, to the crown ether is the driving force in the origin of a complex precessional motion, since the DABCOH$_2^{2+}$ unit is forcefully tilted with respect to its rotation axis, causing a fast and reversible transition from a tetragonal to a monoclinic symmetry that affects the birefringence of the crystals (see Figure 1).

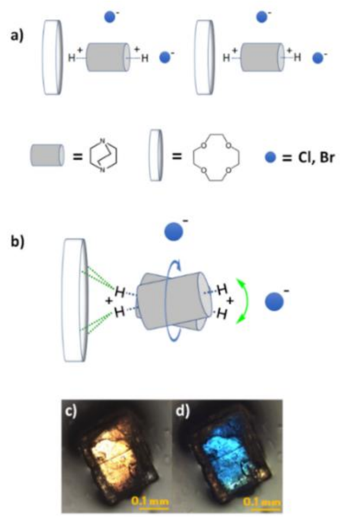

Figure 1. a) Building blocks composing [(12-crown-4)·DABCOH$_2$](X)$_2$ (X=Cl, Br); b) pictorial representa ion of the precessional motion; c) and d) optical photographs under polarized light of a crystal of [(12-crown-4)·DABCOH$_2$](Br)$_2$ below and above Tc respectively.

[a] Dr. L. Fornasari, Dr. S. d'Agostino, Prof. D. Braga
Dipartimento di Chimica G. Ciamician, Università di Bologna
Via Selmi, 2, 40126 Bologna, Italy
simone.dagostino2@unibo.it
[b] Dr. A. Olejniczak, Prof. Andrzej Katrusiak
Adam Mickiewicz University, Faculty of Chemistry, Umultowska 89b, 61-614 Poznań, Poland.
katran@amu.edu.pl
[c] Dr F. Rossi, Prof. M. R. Chierotti, Prof. R. Gobetto
Department of Chemistry and NIS Centre, University of Torino
Via Giuria 7, 10125 Torino, Italy
michele.chierotti@unito.it

Supporting information for this article is given via a link at the end of the document.

In this framework the rotational dynamics of a typical rotor can be schematized as a multiple-well potential energy curve in which the energy barriers are defined by the interplay of steric repulsion, electronic factors and electrostatic interactions, as well as by the conformational flexibility of the cation. The motion is therefore activated or deactivated by thermal energy. In this regard, the application of pressure to the system offers a promising approach to the modulation of the potential energy curve, owing to the fact that both the packing density and the weak interactions are profoundly affected by pressure.[22][23] It is often assumed that pressure and temperature are in an inverse relation, i.e. the effect of the high pressure is comparable to that of a low temperature, but this does not necessarily hold, especially in crystals possessing anisotropic compressibility.[24][25] In the present work we describe the dynamics of the supramolecular complexes [(12-crown-4)$_2$·DABCOH$_2$](X)$_2$ (X=BF$_4$, ClO$_4$) (see Scheme 1), that are in fact an iteration of the design principles adopted previously.[21] Herein complexity is added to the system using tetragonal instead of spherical anions; as a result, discrete structural units are formed, that self-assemble in a chiral structure. The solids were investigated by a combination of XRD techniques, solid-state NMR and thermal analyses, showing that both the DABCOH$_2^{2+}$ cations and the crown ethers undergo fast rotational motions. Furthermore, the structure determination of [(12-crown-4)$_2$(DABCOH$_2$)](BF$_4$)$_2$ at high pressure was performed through single-crystal XRD experiments in a Diamond Anvil Cell (DAC). The analysis of the high-pressure structural features combined with the ambient-pressure crystallographic and spectroscopic evidences elucidate a geared rotational motion between the 12-crown-4 ethers: complete up/down motion of the methylene bridges is hampered and the ethers are locked in a chiral conformation, resembling the macroscopic functioning of meshed spiral gears. Despite the peculiarity of the chosen model compound, we believe that the results are of general interest, pointing out that pressure is a crucial variable in the modulation of the dynamic properties of molecular rotors in the solid state.

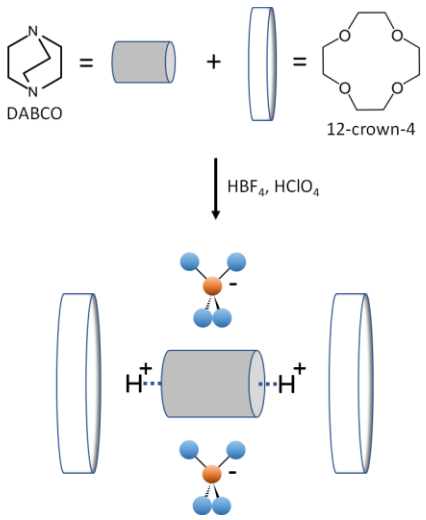

Scheme 1. Building blocks composing [(12-crown-4)$_2$·DABCOH$_2$](X)$_2$ (X=BF$_4^-$, ClO$_4^-$).

Results and Discussion

Crystal structures description

[(12-crown-4)$_2$(DABCOH$_2$)](BF$_4$)$_2$ and [(12-crown-4)$_2$(DABCOH$_2$)](ClO$_4$)$_2$ are isomorphous; they crystallize in the trigonal enantiomeric space groups P3$_1$2$_1$ or P3$_2$2$_1$ and form colorless block-like crystals. The crystal packing is defined by the repetition of discrete units comprising a doubly-protonated DABCO molecule coordinating two crown-ethers as represented in Figure 2. Coordination is achieved through charged-assisted N-H···O hydrogen bonds, additionally each DABCOH$_2^{2+}$ cation is surrounded by four anions (see Figure 2 and Table SI-4 for a list of the distances).

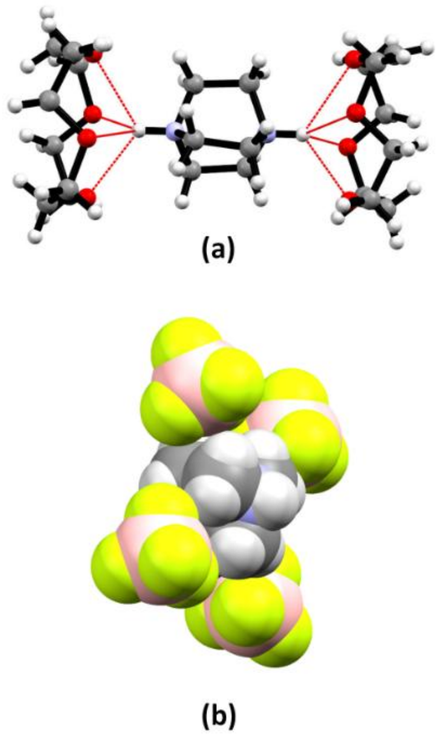

Figure 2. a) The discrete unit (12-crown-4)$_2$(DABCOH$_2$) in the crystals of [(12-crown-4)$_2$(DABCOH$_2$)](BF4)$_2$ and [(12-crown-4)$_2$(DABCOH$_2$)](ClO$_4$)$_2$; b) space-filling representation of the DABCOH$_2^{2+}$ cation surrounded by four BF4$^-$ anions.

All the components at room temperature are disordered. The anions are characterized by an almost plastic behaviour,[26][17] hampering the precise location of the atomic positions. The DABCOH$_2^{2+}$ cations exhibit disorder of C-atoms, likely due to the motion of the dication around its pseudo-threefold axis. Three crystallographically non-equivalent positions were refined for each C-atom; in both cases one of those partitions accounted for a higher occupancy (40-50%).

The crown ethers show a conformational disorder (Figure 3-b) with the respective occupancies not evenly distributed, the ratio is approximately 70/30 in [(12-crown-4)$_2$(DABCOH$_2$)](BF$_4$)$_2$ and 65/35 in [(12-crown-4)$_2$(DABCOH$_2$)](ClO$_4$)$_2$.

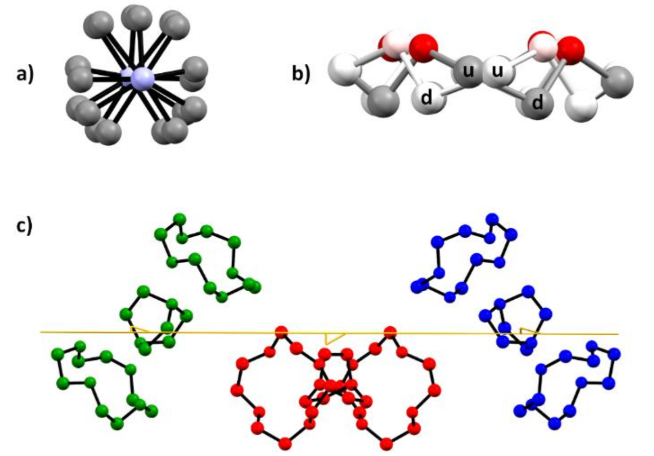

Figure 3. a) Ball and stick model of the disordered positions of the $DABCOH_2^{2+}$ cation observed in the RT structure (H-atoms omitted for clarity); b) the two conformations of the 12-crown-4 ether; c) disposition of the (12-crown-4)$_2$($DABCOH_2$)$^{2+}$ units along he 3_1 axis (marked in yellow); each unit is depicted in a different color.

Low temperature data were collected at 200 K and 100 K. The space group is preserved throughout the entire range from room temperature to 100 K, and no phase transitions were detected in the attainable range from DSC measurements (see Figure SI-8 and SI-9). At 200 K and 100 K the $DABCOH_2^{2+}$ cations undergo partial ordering: distinct split positions for the C-atoms were not easily identified from the electron density, even though the ellipsoids still show elongation along the tangential direction, thus suggesting that a dynamic process (see Figure SI-2) is still ongoing. Similar considerations can be made for the anions, except split positions for the F atoms could be refined at 200 K that account for roughly 15-20% of the occupancy. The crown ethers at low temperature show traces of disorder, however the electron density accounting for the enantiomeric conformation is significantly lower (<8% occupancy), so that the refinement of the independent positions was unsuccessful. On the other hand, at 360 K, the ratio in occupancy for the two conformations of the crown ethers changes to a value of 40/60. Interestingly, in both cases, the initial 70/30 ratio is restored after going back to RT. These observations suggest that that the two conformations might interconvert depending on the temperature. According to literature on crown ethers,[27][28][29] their overall dynamics are often the result of two motions occurring independently and at slightly different rates. The first one corresponds to the up-down inversion of the CH_2-CH_2 bridges,[28] while in the second one, the whole molecule rotates on its molecular pseudo-four-fold axis so that each OCH_2-CH_2 unit "jumps" to adjacent sites every $\pi/2$. Concerning the first motion X-ray diffraction studies are able to determine the population occupancy of the two conformations, but the possible dynamics could not be assessed only by XRD techniques: since the second motion is diffraction invisible, this prompted us to perform solid-state NMR measurements to gain more insights into the dynamics of these systems (see next section).

Solid State NMR – Dynamics

^{13}C MAS spectra of [(12-crown-4)$_2$·$DABCOH_2$](ClO_4)$_2$ and [(12-crown-4)$_2$·$DABCOH_2$](BF_4)$_2$ at room temperature (Figure 4) show two signals at 45.5 and 65.2 ppm assigned to the CH_2 groups of ($DABCOH_2$)$^{2+}$ and 12-crown-4 ether, respectively.

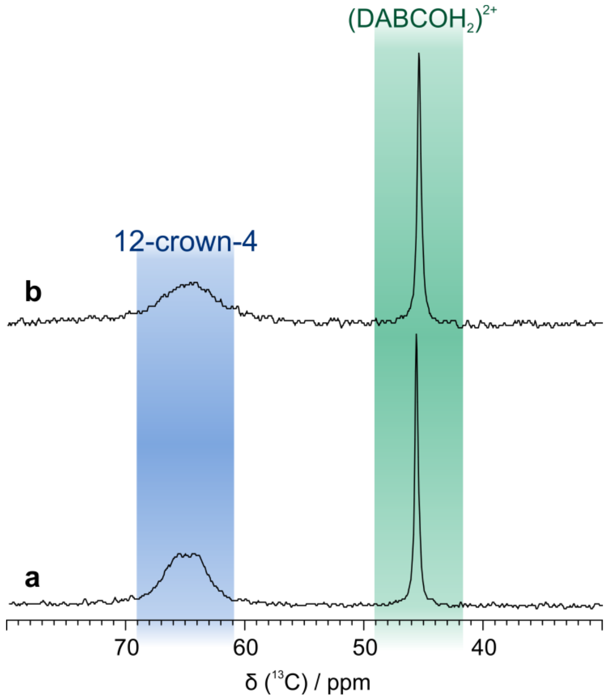

Figure 4. Room temperature ^{13}C (150.9 MHz) MAS SSNMR spectra of a) [(12-crown-4)$_2$·$DABCOH_2$](ClO_4)$_2$ and b) [(12-crown-4)$_2$·$DABCOH_2$](BF_4)$_2$, acquired at a spinning speed of 20 kHz.

To understand the dynamical processes present in the supramolecular salt, variable temperature (VT) NMR measurements were also performed. ^{13}C MAS spectra of [(12-crown-4)$_2$·$DABCOH_2$](ClO_4)$_2$ obtained at different temperature values, from 213 to 353 K, are reported in Figure 5. By changing the temperature, the ($DABCOH_2$)$^{2+}$ signal does not show any difference. This is due to the well-known fast rotation of the DABCO unit along its pseudo-three-fold axis, which is associated with a very low activation energy.[30][31][32] Such motion cannot be frozen at the lowest achievable NMR temperature and thus its effect is not observed in the ^{13}C MAS spectra. On the other hand, the signal at higher ppm shows two different resonances (64.3 and 65.8 ppm) at high temperatures, which then coalesce and merge into one as the temperature is lowered. The coalescence temperature is around 293 K and an activation energy of 58.4 kJ·mol^{-1} evaluated by lineshape analysis is obtained.

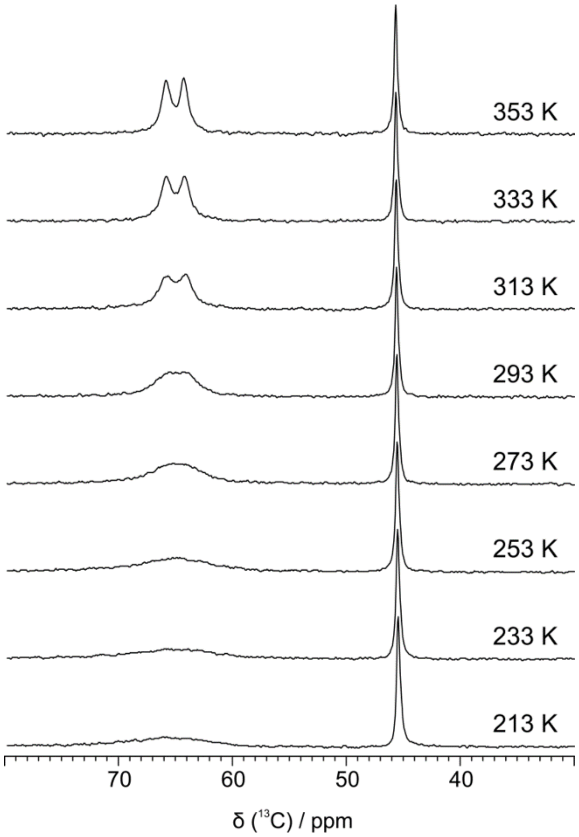

Figure 5. VT ^{13}C (150.9 MHz) MAS SSNMR spectra of [(12-crown-4)$_2$·DABCOH$_2$](ClO$_4$)$_2$ acquired at a spinning speed of 20 kHz.

We surmise that the difference in the CH_2 resonances at high temperature is probably due to the four "up" and four "down" CH_2 groups, independently from the conformational occupancy. This implies that, in these systems, the "up" and "down" motion, if present, is much slower than the NMR time scale.

At low temperature, the signal of the crown ether becomes broader and almost fades out. Two possible mechanisms have been proposed to explain this behavior: (i) for nuclei which have the anisotropic chemical shift as their main static broadening interaction, random molecular motion interferes with magic angle spinning and the maximum broadening is reached when the motional jump rate is equal to the spinning rate; and (ii) for nuclei whose main principal line broadening is due to heteronuclear dipolar coupling, molecular motion (i.e. crown rotation) destructively interferes with decoupling field, rendering it ineffective. [29][33] Since, for CH_2 groups, dipolar coupling is by far the strongest interaction, we surmise that the second mechanism is taking place as the source of line broadening. The same behavior is observed for [(12-crown-4)$_2$·DABCOH$_2$](BF$_4$)$_2$, for which an higher activation energy is found (Figure SI-6 in the Supporting Information).

To get deeper insights into the dynamic, a wide-line quadrupolar echo ^{2}H NMR analysis was carried out on the synthesized deuterium analogous of [(12-crown-4)$_2$·DABCOH$_2$](ClO$_4$)$_2$, prepared by perdeuterated DABCO. In fact, it is well-known that ^{2}H lineshape is highly affected from different kinds of motion and thus is considered a valuable tool to investigate dynamics.[34] Figure 6 shows the VT wide-line ^{2}H SSNMR spectra in the 193-293 K range; however, no appreciable change in the lineshape is observed. This is in good agreement with the very low activation energy associated with the high rotational frequencies of the DABCO unit around its principal axis, already discussed above. This motion is therefore confirmed to be the only dynamic process present in the supramolecular salt, involving the DABCO unit.

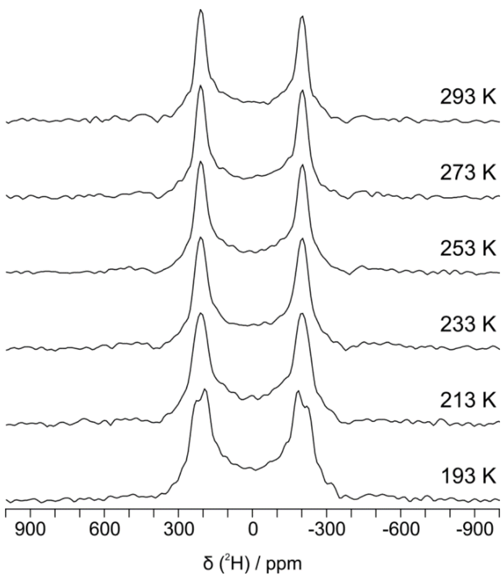

Figure 6. VT wide-line ^{2}H (92.1 MHz) SSNMR spectra of [(12-crown-4)$_2$·DABCOH$_2$](ClO$_4$)$_2$ acquired under static condition.

High-pressure experiments

Crystals of [(12-crown-4)$_2$·DABCOH$_2$](BF$_4$)$_2$ were compressed at isothermal conditions and the structural changes were monitored by single-crystal XRD. A comparison of the relative compression of the unit cell parameters with increasing pressure and decreasing temperature shows that the same level of compression observed at 100 K is achieved already at 0.3 GPa (see Figure 7). The work component of Gibb's free energy on compression by 0.3 GPa at 296 K equals 1.8 kJ·mol^{-1}, compared to the entropy drop on cooling the crystal to 100 K at 0.1 MPa, estimated from Boltzmann's equation as $k_B \cdot \Delta T$=1.7 kJ·mol^{-1}. This comparison reflects the similar effects of complex monotonic changes induced by pressure and temperature, which include the interplay of shortening of intermolecular contacts and reduced vibrations in the structure. Noteworthy, in the 0.1 MPa-0.3 GPa range, the linear compression of parameter *a* is larger than that of parameter *c*, and the thermal expansion of *a* is larger than that of *c*, too, in agreement with the rule of reverse pressure and temperature effects.[25] However, above 0.3 GPa the strongly nonlinear compression of *a* becomes smaller than that of *c*, which is an indication that the mechanisms of structural changes induced by pressure are considerably different than those in the crystal cooled to 100 K. It is connected with the considerably smaller crystal volume above 0.3 GPa, and consequently stronger intermolecular/interionic interactions. Indeed, a qualitative analysis of the thermal parameters of the high-pressure structures in comparison with the 100 K structural model reveals significant differences (see Figures SI-2 and SI-3). The ellipsoids of the DABCO C-atoms are markedly elongated along the tangential direction, suggesting that the rotational motion is retained. Disordered positions for the crown ethers could be traced in the electron density residuals, however, the refinement of the distinct positions of the two enantiomeric conformations was unsuccessful. This may be related to the low fraction of the minor conformation or to the lower quality of the high-pressure data. On the other hand, the high pressure efficiently eliminates structural disorder, strongly hampered in confined spaces. The non-linear thermal expansion of lattice parameters results of the damping of non-harmonic processes, such as rotations, large-amplitude vibrations and even conformational conversions in the structure.

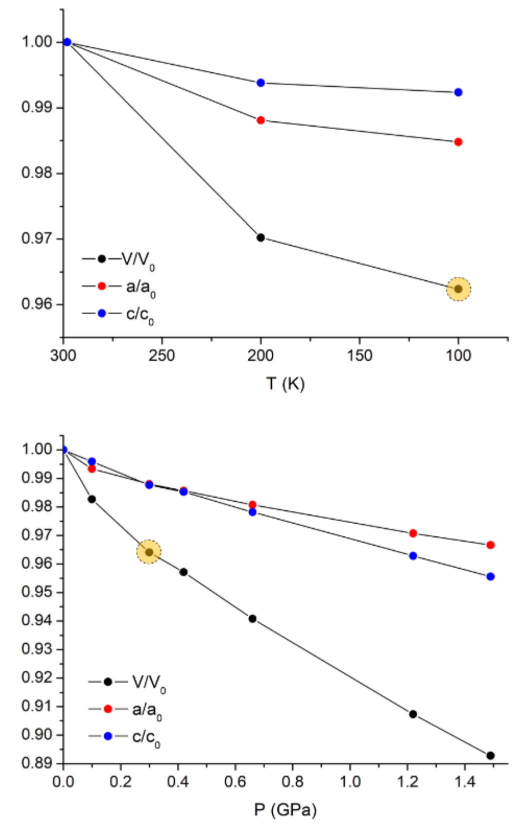

Figure 7. Relative compression of the cell parameters of [(12-crown-4)$_2$·DABCOH$_2$](BF$_4$)$_2$ as a function of temperature (top) and pressure (bottom). Yellow spots indicate the same level of compression observed at 100 K and at 0.3 GPa.

Relevant intermolecular distances were monitored as a function of pressure. Given the disorder affecting the structures the choice was made as explained in the following to ensure that comparable values could be extrapolated in the different experimental conditions. To probe the surroundings of the DABCOH$_2^{2+}$ cations, charge assisted N-H···O bonds with the crown ether and the distance between the DABCO centroid along the N-N axis and the B-atom of the anions were selected. The distance between crown ethers was monitored through the O···O distance of neighboring rings; every ether is indeed surrounded by other four molecules of crown ether, as described in Scheme SI-1, two lay in the same plane in antiparallel fashion and two are perpendicular to the O-atom plane.

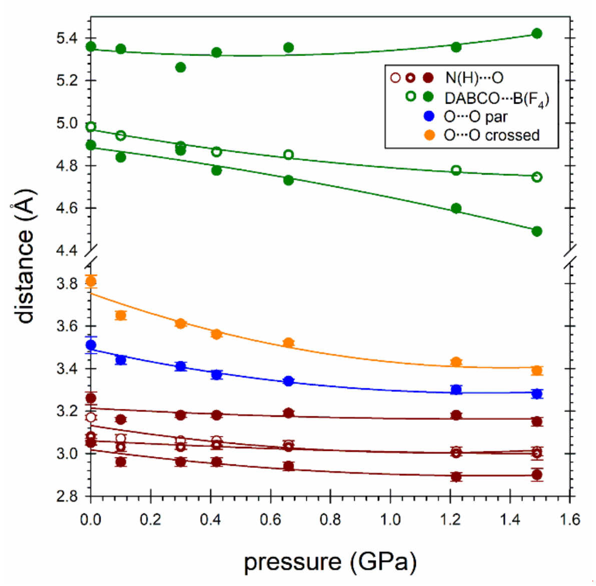

Figure 8. Intermolecular distances of [(12-crown-4)$_2$·DABCOH$_2$](BF4)$_2$ as a function of pressure (cf. Scheme SI-1 and Table SI-4). The estimated standard devia ions (ESDs) of the plotted values are either smaller or comparable to the size of the symbols, as indicated by errorbars, while all ESDs of pressure are 0.02 GPa and have been omitted.

The results are summarized in Table SI-4 and Figure 8. Interestingly, the N-H···O bonds are roughly unaltered both at low temperature and pressure up to 1.5 GPa, coherently to the fast dynamics established by the NMR analysis. Of the four anions surrounding every DABCOH$_2^{2+}$ cation, one has a significantly longer distance. This is expected to be less interacting with the cation and its distance shows a pronounced discontinuity: it is reduced up to 0.3 GPa and grows again at higher pressure. Notably, the space group symmetry is conserved upon displacement of the anions. Finally, the distance between neighboring crown ethers is reduced at both low temperature and high pressure, as expected since they are the bulkiest building blocks; however, the thermal parameters at 0.66 GPa do not hint at any reduction in the dynamics (see Figure SI-3).
We suggest therefore that the rotational motions are maintained within the crystal packing thanks to their correlation. It is evident from Figure 9-a that the conformations of the antiparallel crown ethers are correlated: an exchange of the up/down positions of one of the two molecules would be impossible without a structural rearrangement for steric reasons; the two molecules are thus locked and must rotate in a concerted manner. Similarly, the steric hindrance of the CH$_2$ groups in the “crossed” arrangement (Figure

9-b) would obstruct the rotation of one crown ether if the other one was stationary.

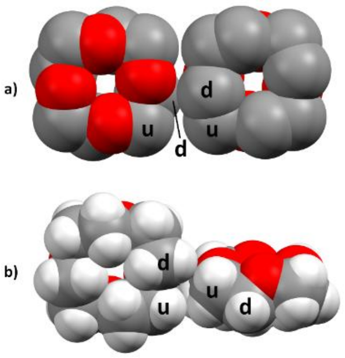

Figure 9. Space filling structure of the neighbouring crown ethers in an iparallel arrangement (at 0.42 GPa) (a) and "crossed" arrangement (b); H-atoms are omitted in (a) for clarity.

In this case, though, it is difficult to determine if the handeness of the crown ether is a critical factor. In this picture, the chiral 12-crown-4 ethers can be compared from the functionality standpoint to spiral gears that must possess matching handedness in order to mesh. This could account for the finding that the CH_2 motion is strongly hindered, since an inversion of the handedness of one crown ether must be concomitant with the inversion of the ethers meshed with it, as depicted in Figure 10, which is statistically less likely to happen.

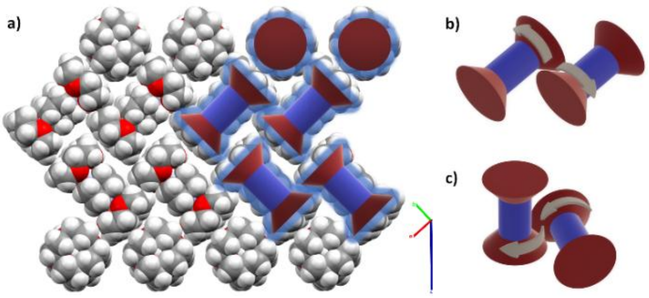

Figure 10. Crystal packing of the $[(12\text{-crown-}4)_2{\cdot}DABCOH_2]^{2+}$ units (a) highlighting correlation between adjacent crown ethers (anions omitted for clarity) and schematics of the proposed geared motion between antiparallel (b) and perpendicular (c) ethers.

At pressure higher than 1.55 GPa, the experimental evidence (Figure 11) is consistent with a collapse-type transition to a lower-symmetry phase (hereafter referred to as phase II) that could not be obtained at the temperature as low as 100 K. The strain generated by the symmetry reduction, most likely to a triclinic lattice, resulted in the sample twinning and hampered the structure determination of phase II. The transition occurs when the crystal is compressed to nearly 90% of the ambient-pressure volume, which must have resulted in a considerable increase of intermolecular interactions. Therefore, it is highly unlikely that any dynamic disorder persists to this pressure point. A likely reason for the transition can be collapses of small voids formed in the structure due to the presence of directional interactions, for example the charge assisted hydrogen bonds N-H···O between cations $DABCOH_2^{2+}$ and crown-ether molecules. The work-component of Gibb's free energy at 1.55 GPa is of nearly 40 kJ·mol^{-1}, which corresponds to the energy of charge assisted hydrogen bonds N-H···O in this structure. Thus, it is natural to expect that these H-bonds bend under this compression and that the structure transforms toward the more densely-packed arrangement. The discontinuities in the lattice parameters indicate that the transition is of 1st order according to Ehrenfest's classification, consistently with the suggested scenario of H-bonds yielding under stress and the structure collapsing to a more compact arrangement.

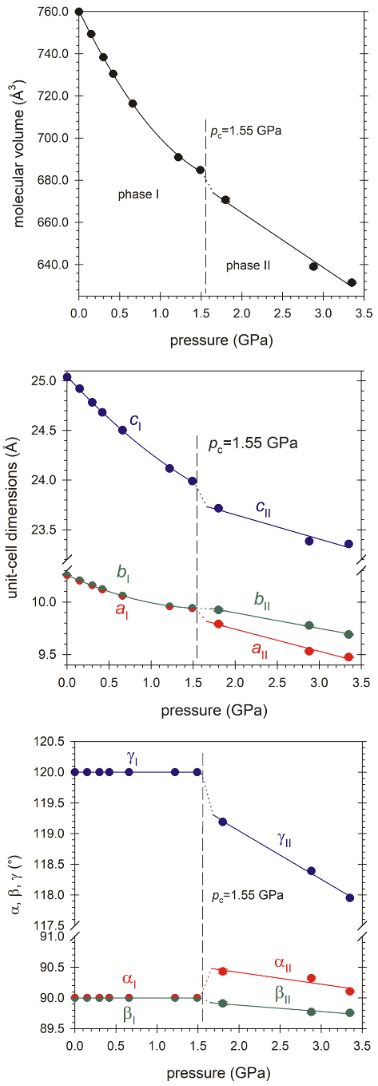

Figure 11. The pressure dependence of he unit-cell dimensions (molecular volume Vm calculated as V/Z); the dashed lines indicate the pressure-induced phase transition at pc=1.55 GPa. The dotted lines close to pc are for guiding the eye only. ESDs of the parameters are all smaller than the plotted symbols, while all ESDs of pressure are 0.02 GPa and have been omitted.

Conclusions

Crystals possessing components in rapid motion are at the forefront of the research on solid-state molecular machines. The common approach envisages the modification of the molecular dynamics by acting on the thermal parameters alone. The final goal would be the development of stimuli-responsive materials based on molecular rotors. In view of this, it would be highly desirable to be able to utilize also mechanical parameters, namely pressure and volume, to control motion on the molecular scale. With this in mind, we have reported here the results of our studies on the solid-state dynamics of the supramolecular salts of general formula $[(12\text{-crown-}4)_2\cdot DABCOH_2](X)_2$ (where X=BF_4, ClO_4), as a function of temperature and pressure, through the combination of variable temperature and variable pressure XRD techniques and variable temperature ^{13}C and ^{2}H solid-state NMR spectroscopy. To the best of these authors' knowledge, this is the first time that the effect of pressure is deliberately investigated in the context of artificial molecular rotors.

The salts $[(12\text{-crown-}4)_2\cdot DABCOH_2](X)_2$ are isostructural, and all the building blocks composing the supramolecular complex display dynamic processes at ambient temperature and pressure. However, the interconversion between the two enantiomerically-related conformations of the crown ethers is strongly hampered, accounting for the lack of an inversion center. Whereas the dynamics of the crown ethers are attenuated at low temperature through a monotonic thermal compression of the lattice, the structural disorder of the salts is substantially unaffected upon monotonic pressure-induced compression.

Therefore, we have argued that the motion of the crown ethers is maintained thanks to the correlation between neighboring molecules that mesh and rotate in a concerted manner similarly to spiral gears, with pressure acting like the mean to couple and decouple the gears.

Above 1.55 GPa, the experimental evidences are consistent with a collapse-type transition to a lower-symmetry ordered structure, that could not be obtained at a temperature as low as 100K, providing further confirmation that the inverse relationship between temperature and pressure effects on molecular motion in the solid state does not hold.

Experimental Section

All the reagents and solvents were obtained from commercial sources and used as received.

CAUTION: perchlorate salts are potentially explosive and should be handled with extreme care.[35]

Synthesis

$[(12\text{-crown-}4)_2(DABCOH_2)](BF_4)_2$ and $[(12\text{-crown-}4)_2(DABCOH_2)](ClO_4)_2$ were prepared according to the following general procedure: DABCO was dissolved in deionized water along with 2 equivalents of the crown ether. An aqueous solution of HBF_4 or $HClO_4$ was added dropwise until neutralization and after few hours a white solid precipitated from the solution. The solid was thus filtered and washed with ethanol. The bulk product was characterized by XRPD, while crystals suitable for single-crystal and high-pressure experiments were obtained by recrystallization of the precipitated materials in dimethylformamide.

High-pressure experiments

All the experiments were performed in a Merrill-Bassett diamond anvil cell (DAC) modified by supporting the anvils directly on steel discs with a conical window (type 1A diamonds, cutlet size 0.8 mm). Steel gaskets of thickness 0.25 mm were employed for $[(12\text{-crown-}4)_2(DABCOH_2)](BF_4)_2$, the diameter of the holes was 0.4 mm. Pressure in the DAC was cal brated by the ruby fluorescence method[36][37] with a Photon Control spectrometer affording the 0.02 GPa precision. A single crystal of $[(12\text{-crown-}4)_2(DABCOH_2)](BF_4)_2$ was stuck on one anvil of the DAC with immersion oil, then the chamber was filled with Daphne oil, sealed and the pressure was increased in steps (see Figure SI-11). After every step the crystal data were collected.

Ambient pressure SCXRD

Single-crystal data for $[(12\text{-crown-}4)_2(DABCOH_2)](BF_4)_2$ and $[(12\text{-crown-}4)_2(DABCOH_2)](ClO_4)_2$ were collected on an Oxford Diffraction Xcalibur S CCD diffractometer equipped with a graphite monochromator (Mo-Kα radiation, λ = 0.71073 Å), and with a cryostat Oxford CryoStream800. The structures were solved by intrinsic phasing with SHELXT[38] and refined on F^2 by full-matrix least squares refinement with SHELXL implemented in Olex2 software.[39] The refinements against the room-temperature data were performed according to the following procedure: the DABCO C-atoms were split into three positions, whereas O and C-atoms of the crown ethers and F-atoms or Cl-atoms of the anions were split into two positions. Occupancies of all the conformations were refined independently for the anisotropic model and fixed upon convergence. Due to the high number of parameters, anisotropic refinements were performed applying EADP constraints to the thermal parameters of DABCO and crown ethers. Finally, H-atoms of the crown ethers and DABCO N-atoms were placed in calculated position and refined with a riding model. For low-temperature data all non-H atoms were refined anisotropically, while H-atoms were placed in calculated position and refined with a riding model.

High-pressure SCXRD

The diffraction data were collected on a Kuma diffractometer with Mo Kα radiation (λ=0.71073 Å) equipped with a CCD detector. CrysAlisPro 171.37.31 was used for recording reflections[40] and preliminary data reduction. The intensities were corrected for the effects of DAC absorption, diamond diffraction and sample shadowing by the gasket. The crystal structure of $[(12\text{-crown-}4)_2(DABCOH_2)](BF_4)_2$ determined at ambient-pressure 100K was used as the starting model refined against high-pressure data, on F^2 by full-matrix least squares refinement with SHELXL implemented in Olex2 software.[39] Two disordered positions were assigned to the F-atoms of the BF4 anions; their occupancy refined in the anisotropic model and then fixed for the final refinement. All non-H atoms were refined anisotropically. H-atoms were located at ideal positions and included in the refinements riding on their carriers.

The crystal data and refinements details are summarized in Tables SI-1, SI-2, and SI-3; the experimental and structural details have been deposited in the CIF form in the Cambridge Structural Database, Nos. 1973341-1973354.

Powder XRD

For phase identification, X-ray powder diffraction diffractograms were collected on a PANalytical X'Pert Pro automated diffractometer equipped with an X'Celerator detector in Bragg–Brentano geometry, using Cu–Kα radiation (λ = 1.5418 Å) without monochromator in the 2θ range between 3° and 50° (continuous scan mode, step size 0.0167°, counting time 19.685 s, Soller slit 0.04 rad, antiscatter slit ½, divergence slit ¼, 40 mA*40kV). The program Mercury[41] was used for simulation of X-ray powder patterns on the basis of single crystal data. In all cases, the identity between polycrystalline samples and single crystals was always verified by comparing experimental and simulated powder diffraction patterns (See Figures ESI-4 and ESI-5).

Thermal analyses

TGA analyses were performed with a Perkin-Elmer TGA-7. Each sample, contained in a platinum crucible, was heated in a nitrogen flow (20 $cm^3 \cdot min^{-1}$) at a rate of 5°C·min^{-1}, up to decomposition. Samples weights were in the range 5–10 mg.

Calorimetric measurements were performed with a Perkin-Elmer DSC-7 equipped with a PII intracooler. Temperature and enthalpy calibrations were performed using high-purity standards (n-decane, benzene and indium). Heating of the aluminium open pans containing the samples (3 – 5 mg) was carried out at 5 °C·min^{-1} in the temperature range -30 – 200°C.

Solid-State NMR

^{1}D ^{13}C MAS and ^{2}H static SSNMR spectra were acquired on a Jeol ECZR 600 instrument, operating at 600.2, 150.9 and 92.1 MHz for the ^{1}H, ^{13}C and ^{2}H nuclei, respectively. Powder samples were packed in 3.2 mm diameter cylindric zirconia rotors with a volume of 60 μL. A certain amount of sample was taken and used without further preparation from each batch to fill the rotor. ^{13}C MAS spectra were acquired at a spinning speed of 20 kHz with a 90° ^{13}C pulse of 2.15 μs, a recycle time of 20 s and 32 scans. The two-pulse phase modulation (TPPM) decoupling scheme with a 116.0 kHz radiofrequency field was used. ^{2}H wide-line spectra were recorded with a 90° 2H pulse of 3.0 μs and 32 scans. To acquire the ^{2}H wide-line spectra, a quadrupolar-echo pulse sequence with an echo delay of 5 μs and recycle delay of 5 s was employed. 13C chemical shifts were referenced to glycine (^{13}C methylene signal at 43.5 ppm). Variable-temperature operation was achieved by a triple gas channel MAS probe, in which the stream of VT gas is separated from the MAS bearing and driving gases. The driving gas is used to propel the rotor at high speeds, while the bearing gas provides an air cushion for stability. The low temperatures were achieved by cooling the VT line through a flow of boil-off N_2 gas from an exchange Dewar filled with liquid nitrogen. The VT gas was then directed at the mid-point of the sample rotor. For the high temperature operations, VT and MAS gases were air heated by means of a resistance put inside the probe. A thermocouple was used for temperature measurement and regulation. The temperature was cal brated using the well-established method based on the ^{207}Pb NMR resonance of solid $Pb(NO_3)_2$.[42] [43] [44]

Acknowledgements

Financial support by the Universities of Bologna, and Torino and from the Adam Mickiewicz University is gratefully ackowledged. F.R. thanks Jeol (Italia) S.p.A. for a Ph.D. scholarship. L. F. was a Ph.D. visiting student at Adam Mickiewicz University thanks to a Marco Polo scholarship granted by the Department of Chemistry "G. Ciamician."

Keywords: • Dynamic processes in Crystals Non-Ambient Crystallography • VT Solid-State NMR

[1] D. Braga, F. Grepioni, L. Maini, S. d'Agostino, *Eur. J. Inorg. Chem.* **2018**, *2018*, 3597–3605.

[2] D. Braga, *Chem. Rev.* **1992**, *92*, 633–665.

[3] J. D. Dunitz, V. Schomaker, K. N. Trueblood, *J. Phys. Chem.* **1988**, *92*, 856–867.

[4] J. Painter, E. A. Merritt, *Acta Crystallogr. Sect. D Biol. Crystallogr.* **2006**, *62*, 439–450.

[5] H. B. Burgi, *Annu. Rev. Phys. Chem.* **2000**, *51*, 275–296.

[6] W. I. F. David, R. M. Ibberson, T. J. S. Dennis, J. P. Hare, K. Prassides, *Epl* **1992**, *18*, 735–736.

[7] R. Tycko, G. Dabbagh, R. M. Fleming, R. C. Haddon, A. V. Makhija, S. M. Zahurak, *Phys. Rev. Lett.* **1991**, *67*, 1886–1889.

[8] A. Gavezzotti, M. Simonetta, *Chem. Rev.* **1982**, *82*, 1–13.

[9] A. Katrusiak, M. Szafranski, *Phys. Rev. Lett.* **1999**, *82*, 576–579.

[10] S. Bracco, F. Castiglioni, A. Comotti, S. Galli, M. Negroni, A. Maspero, P. Sozzani, *Chem. - A Eur. J.* **2017**, *23*, 11210–11215.

[11] S. Bracco, M. Beretta, A. Cattaneo, A. Comotti, A. Falqui, K. Zhao, C. Rogers, P. Sozzani, *Angew. Chemie - Int. Ed.* **2015**, *54*, 4773–4777.

[12] W. Setaka, K. Yamaguchi, *Proc. Natl. Acad. Sci.* **2012**, *109*, 9271–9275.

[13] K. M. Hutchins, R. H. Groeneman, E. W. Reinheimer, D. C. Swenson, L. R. MacGillivray, *Chem. Sci.* **2015**, *6*, 4717–4722.

[14] D. R. Islamov, V. G. Shtyrlin, N. Y. Serov, I. V. Fedyanin, K. A. Lyssenko, *Cryst. Growth Des.* **2017**, *17*, 4703–4709.

[15] C. S. Vogelsberg, M. A. Garcia-Garibay, *Chem. Soc. Rev.* **2012**, *41*, 1892–1910.

[16] S. d'Agostino, L. Fornasari, F. Grepioni, D. Braga, F. Rossi, M. R. Chierotti, R. Gobetto, *Chem. - A Eur. J.* **2018**, *24*, 15059–15066.

[17] S. D'Agostino, L. Fornasari, D. Braga, *Cryst. Growth Des.* **2019**, *19*, 6266–6273.

[18] A. Comotti, S. Bracco, P. Sozzani, *Acc. Chem. Res.* **2016**, *49*, 1701–1710.

[19] X. Jiang, Z. J. O'Brien, S. Yang, L. H. Lai, J. Buenaflor, C. Tan, S. Khan, K. N. Houk, M. A. Garcia-Garibay, *J. Am. Chem. Soc.* **2016**, *138*, 4650–4656.

[20] M. E. Howe, M. A. Garcia-Garibay, *J. Org. Chem.* **2019**, *84*, 9835–9849.

[21] S. d'Agostino, L. Fornasari, F. Grepioni, D. Braga, F. Rossi, M. R. Chierotti, R. Gobetto, *Chem. - A Eur. J.* **2018**, *24*, 15059–15066.

[22] A. Katrusiak, *Acta Crystallogr. Sect. A Found. Crystallogr.* **2008**, *64*, 135–148.

[23] A. Olejniczak, K. Ostrowska, A. Katrusiak, **2009**, 15761–15767.

[24] W. Cai, A. Katrusiak, *Nat. Commun.* **2014**, *5*, 1–8.

[25] J. Marciniak, A. Katrusiak, *J. Phys. Chem. C* **2017**, *121*, 22303–22309.

[26] J. Janikowski, M. R. Razali, S. R. Batten, D. R. MacFarlane, J. M. Pringle, *Chempluschem* **2012**, *77*, 1039–1045.

[27] C. I. Ratcliffe, G. W. Buchanan, J. K. Denike, *J. Am. Chem. Soc.* **1995**, *117*, 2900–2906.

[28] C. I. Ratcliffe, J. A. Ripmeester, G. W. Buchanan, J. K. Denike, *J. Am. Chem. Soc.* **1992**, *114*, 3294–3299.

[29] G. W. Buchanan, A. Moghimi, C. I. Ratcliffe, *Can. J. Chem.* **1996**, *74*, 1437–1446.

[30] L. Catalano, S. Pérez-Estrada, G. Terraneo, T. Pilati, G. Resnati, P. Metrangolo, M. A. Garcia-Garibay, *J. Am. Chem. Soc.* **2015**, *137*, 15386–15389.

[31] L. Catalano, S. Perez-Estrada, H. H. Wang, A. J. L. Ayitou, S. I. Khan, G. Terraneo, P. Metrangolo, S. Browne, M. A. Garcia-Garibay, *J. Am. Chem. Soc.* **2017**, *139*, 843–848.

[32] O. J. Żogał, Z. Galewski, E. Grech, Z. Malarski, *Mol. Phys.* **1985**, *56*, 673–681.

[33] G. W. Buchanan, C. Morat, C. I. Ratcliffe, J. A. Ripmeester, *J. Chem. Soc. Chem. Commun.* **1989**, 1306–1308.

[34] F. H. Larsen, H. J. Jakobsen, P. D. Ellis, N. C. Nielsen, *Chem. Phys. Lett.* **1998**, *292*, 467–473.

[35] D. G. Churchill, *J. Chem. Educ.* **2006**, *83*, 1798–1803.

[36] G. J. Piermarini, S. Block, J. D. Barnett, R. A. Forman, *J. Appl. Phys.* **1975**, *46*, 2774–2780.

[37] H. K. Mao, J. Xu, P. M. Bell, *J. Geophys. Res.* **1986**, *91*, 4673.

[38] G. M. Sheldrick, *Acta Crystallogr. Sect. A Found. Crystallogr.* **2008**, *64*, 112–122.

[39] O. V. Dolomanov, L. J. Bourhis, R. J. Gildea, J. A. K. Howard, H. Puschmann, *J. Appl. Crystallogr.* **2009**, *42*, 339–341.

[40] A. Budzianowski, A. Katrusiak, *High-Pressure Crystallogr.* **2004**, DOI 10.1007/978-1-4020-2102-2.

[41] C. F. Macrae, I. J. Bruno, J. A. Chisholm, P. R. Edgington, P. McCabe, E. Pidcock, L. Rodriguez-Monge, R. Taylor, J. Van De Streek, P. A. Wood, *J. Appl. Crystallogr.* **2008**, *41*, 466–470.

[42] A. Bielecki, D. P. Burum, *J. Magn. Reson. Ser. A* **1995**, *116*, 215–220.

[43] T. Takahashi, H. Kawashima, H. Sugisawa, T. Baba, *Solid State Nucl. Magn. Reson.* **1999**, *15*, 119–123.

[44] X. Guan, R. E. Stark, *Solid State Nucl. Magn. Reson.* **2010**, *38*, 74–76.

Entry for the Table of Contents

FULL PAPER

The solid-state dynamics of the supramolecular salts of formula [(12-crown-4)$_2$·DABCOH$_2$](X)$_2$ (where X=BF$_4$, ClO$_4$) have been investigated as a function of temperature and pressure *via* a combination of non-ambient XRD techniques and VT solid-state NMR spectroscopy.

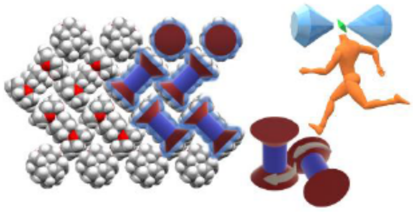

Luca Fornasari, Anna Olejniczak, Federica Rossi, Simone d'Agostino,* Michele R. Chierotti,* Roberto Gobetto, Andrzej Katrusiak,* and Dario Braga.

Page No. – Page No.

Solid-State Dynamics and High-Pressure Studies of a Supramolecular Spiral Gear